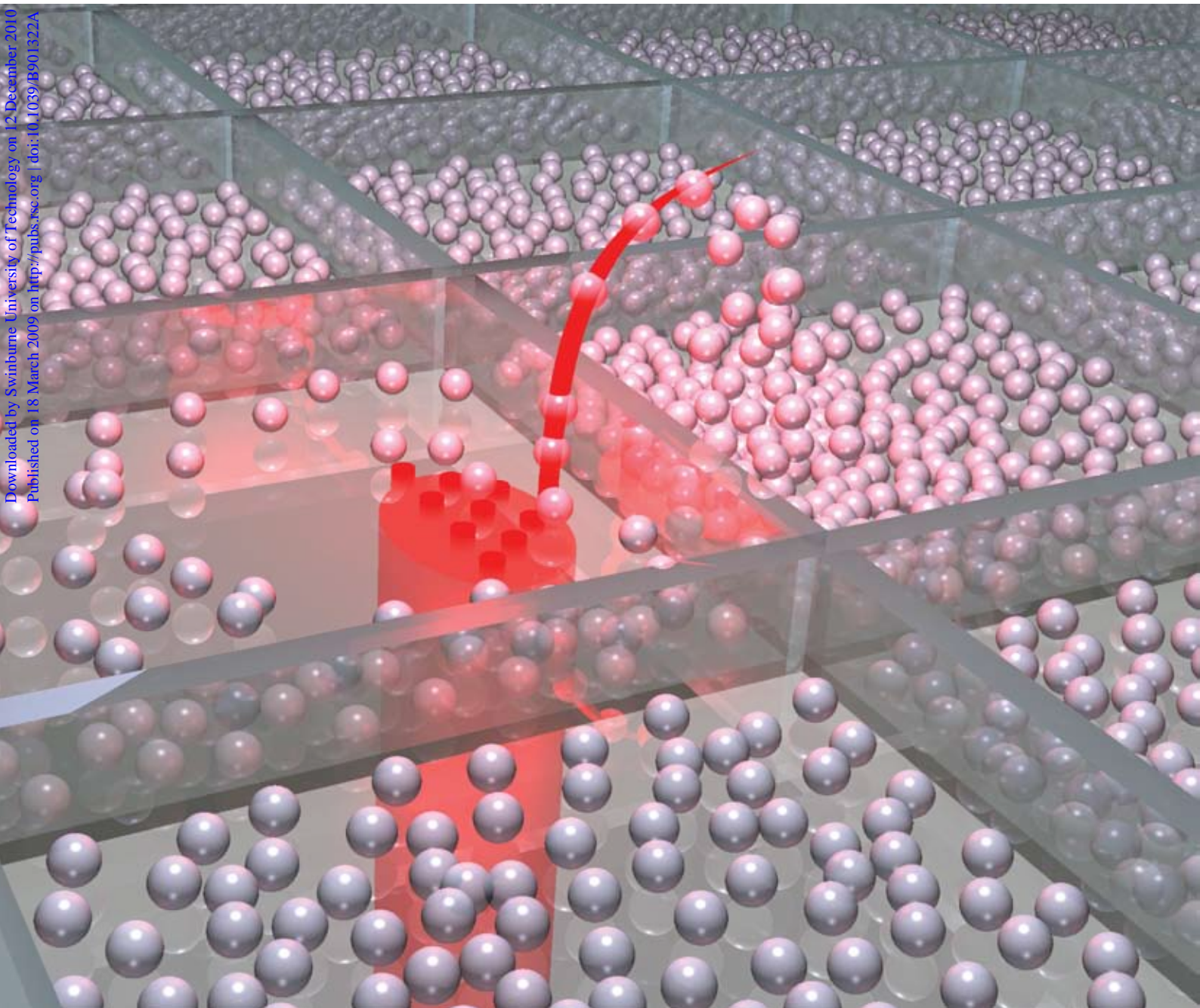


# Lab on a Chip

Miniaturisation for chemistry, physics, biology, & bioengineering

[www.rsc.org/loc](http://www.rsc.org/loc)

Volume 9 | Number 10 | 21 May 2009 | Pages 1309–1480



Downloaded by Swinburne University of Technology on 12-December-2010  
Published on 18 March 2009 on <http://pubs.rsc.org> | doi:10.1039/B901322A

ISSN 1473-0197

RSC Publishing

Baumgartl  
Redistribution of cells between microwells  
Lei  
Travelling wave DEP pump for blood delivery

Charette  
Hybrid interference-absorbance filter  
Qin and Lin  
Microvalve allows precise control of droplets

# Optical redistribution of microparticles and cells between microwells†

Jörg Baumgartl,<sup>\*,a</sup> Gregor M. Hannappel,<sup>a</sup> David J. Stevenson,<sup>a</sup> Daniel Day,<sup>b</sup> Min Gu<sup>b</sup> and Kishan Dholakia<sup>a</sup>

Received 21st January 2009, Accepted 5th March 2009

First published as an Advance Article on the web 18th March 2009

DOI: 10.1039/b901322a

The shaping of laser beams has developed into a powerful tool for optical micromanipulation. In this context, Airy and parabolic laser beams which follow curved trajectories have drawn considerable attention. These beams may allow clearing of microparticles through particle transport along curved paths, a concept termed “optically mediated particle clearing (OMPC).” In this communication we apply this concept to microparticles and cells within specially designed microwells. Our results open novel perspectives for the redistribution of cells between different media within a microfluidic environment.

Optical micromanipulation has evolved into a powerful technique that is applied in several disciplines particularly within a microfluidic environment.<sup>1</sup> Many applications in optical micromanipulation greatly benefit from the use of light fields shaped both in phase and amplitude, including “non-diffracting” laser beams. The most prominent example of a “non-diffracting” laser beam is the Bessel beam<sup>2</sup> which does not spread while propagating, even if the beam diameter is reduced to the size of a tightly focused Gaussian laser beam. Examples of its use include the trapping of particles in multiple microfluidic chambers,<sup>3</sup> the creation of elongated particle conveyor belts<sup>4</sup> and nanotechnology where optically trapped microspheres are used for subwavelength nanopatterning.<sup>5</sup> In biology, Bessel beams have been used for microfluidic cell sorting and the optical transfection of cells.<sup>6</sup> The Airy beam, a second type of “non-diffracting” laser beam, has only recently enriched the field of optical micromanipulation through a basic demonstration of OMPC.<sup>7</sup> This peculiar beam enables particles to follow curved trajectories as opposed to the Bessel beam where particles are guided along a straight line.

In this communication, we apply OMPC in the microfluidic domain by redistributing microparticles and mammalian cells between patterned microwells without the need of microfluidic flow. This opens an alternative route to expose given cell or colloidal samples to various differing environmental media within the same microfluidic chip. An alternative, previous approach to achieve this was based on multiple parallel laminar streams of buffer media combined with optical trapping.<sup>8</sup> Our studies include the first ever use

of parabolic beams, another type of curved “non-diffracting” laser beam, for optical micromanipulation. In addition, we provide a quantitative analysis of the redistribution effect using Airy and parabolic beams. Whilst the majority of experiments were performed on colloidal particles, we also demonstrate the redistribution of red blood cells between microwells. Moreover, we propose a methodology that will allow the redistribution of any cell type.

In our studies, we used Airy<sup>9,10</sup> and parabolic beams,<sup>11,12</sup> a novel family of “non-diffracting” beams discovered only recently. Airy beams consist of a bright main spot and a number of side lobes (left image, in Fig. 1(a)). These beams experience constant transverse acceleration during propagation (see the sequence of transverse beam intensity profiles in Fig. 1(a) from left to right showing the beam’s main spot moving downwards). Zero-order parabolic beams (see Fig. 1(b)) exhibit properties similar to Airy beams except that the beam intensity pattern reduces to a main spot and a single tail of side lobes. This pattern splits up into two main spots and tails for parabolic beams of  $n$ -th order ( $n > 0$ ). The gap is filled by  $n-1$  side tails as shown in Fig. 1(c) and (d) for  $n = 12$  and  $n = 24$ , respectively. In practice the “non-diffracting” properties are only retained for a finite beam propagation distance due to the finite beam intensity. Therefore, both Airy and parabolic beams smear out while propagating.

In our experiments, Airy and parabolic beams were incident from below onto a sample chamber. Due to the optical gradient and scattering forces exerted,<sup>13</sup> particles are dragged into the beam’s main spot across the side lobes and levitated away from the cleared region along curved trajectories. When the beam is smeared out optical forces become weak and, therefore, particles drop out of the beam and sediment back to the sample bottom in a different place from the cleared region. Intuitively, the Airy beam acts as a micrometre-sized snowblower, “blowing” microparticles and cells upwards on an arc-like trajectory.

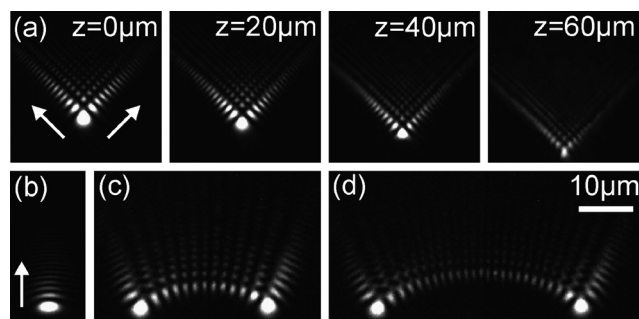


**Fig. 1** (a) Airy beam at different propagation distances  $z$ . (b)–(d) Parabolic beams of different order  $n$  at the propagation distance  $z = 0$ . (b)  $n = 0$ , (c)  $n = 12$ , (d)  $n = 24$ . The white arrows indicate the directions in which particles tend to leave the beam’s main spot as discussed in the text.

<sup>a</sup>SUPA, School of Physics and Astronomy, University of St. Andrews, St. Andrews, Fife, KY16 9SS, UK. E-mail: jb211@st-andrews.ac.uk

<sup>b</sup>Centre for Micro-Photonics, Faculty of Engineering and Industrial Sciences, Swinburne University of Technology, Hawthorn, 3122, Victoria, Melbourne, Australia

† Electronic supplementary information (ESI) available: Video clips showing the redistribution of colloidal particles (clip 1) and red blood cells (clip 2) between two microwells (see caption of Fig. 2 of this communication for details). Full experimental details. See DOI: 10.1039/b901322a

Our experiments were performed using a polarized Ar<sup>+</sup> laser ( $\lambda = 514$  nm). Following the approach presented in ref. 10, a spatial light modulator (SLM) was used to impose a cubic phase modulation onto a Gaussian beam which was subsequently Fourier-transformed into the Airy beam by a spherical lens. The Airy beam was down-sized by an inverse telescope to  $\approx 10$   $\mu\text{m}$  and imaged from below into a sample chamber (1 cm in diameter, 100  $\mu\text{m}$  thick) which consisted of two cover slips separated by a vinyl spacer. The sample contained an aqueous suspension of polymer particles (radius  $R = 2.85$   $\mu\text{m}$ ), heparinised human blood, or Chinese Hamster Ovary cells (CHO) that had phagocytosed polymer spheres ( $R = 1.5$   $\mu\text{m}$ ).<sup>14</sup> Particles and cells were imaged with a 20 $\times$  objective onto a CCD camera, and images were recorded onto a hard disk. Parabolic beams are created in a similar manner to that of Airy beams except that an additional amplitude modulation is required.<sup>12</sup> This modulation reduces the intensity transferred into a parabolic beam by the SLM (approximately 80% less than for an Airy beam). To aid comparison between these light fields, we reduced the Airy beam intensity by 80% using the SLM (see ref. 15 for details). The effective laser powers in the sample plane were 25 mW. Dedicated labview software allowed beam positioning and orientation by simply drawing a line on a recorded image.

The microwell structure was created by coating a negative mold with poly(dimethyl siloxane) (PDMS).<sup>16</sup> A microscope slide was placed on top and the PDMS was cured in an oven at 80  $^{\circ}\text{C}$  for one hour. Afterwards, the microwell structure was peeled off using tweezers and put onto the bottom plate of our sample. The structure comprised 10  $\times$  10 microwells each 100  $\mu\text{m}$   $\times$  100  $\mu\text{m}$  in size. The separating walls had a height of 20  $\mu\text{m}$ .

Human blood was taken and placed into heparinised containers (Becton-Dickinson Vacutainer tubes type NH 170 IU 10 ml). It was diluted 1 : 100 into Hanks Balanced Salt Solution (Sigma, UK) and placed onto either glass coverslips or PDMS microwells. CHO K1 cells were routinely kept in a humidified atmosphere of 5% CO<sub>2</sub>/95% air at 37  $^{\circ}\text{C}$  in Modified Earles Medium (MEM) with 10% foetal calf serum (FCS) (Globepharm, Surrey, UK), 20 enzyme units/ml of penicillin (Sigma, UK) and 20  $\mu\text{g}/\text{ml}$  of streptomycin (Sigma, UK). Cells that had been exposed to polymer spheres ( $R = 1.5$   $\mu\text{m}$ ) for 24 h (Nuncleon, Fisher Scientific, UK) were rendered non-adherent and non-adhesive by suspending in 1 ml trypsin-EDTA (Sigma, UK) throughout the duration of the experiment (<30 min). For PDMS microwell pacification to prevent adhesion, a solution of 20 mg/ml poly-2-hydroxyethylmethacrylate (Sigma, UK) in 95% ethanol was added and allowed to evaporate prior to the addition of the cell solution.<sup>17</sup>

The redistribution of microparticles and cells between microwells requires a careful choice of both the laser power and the laser operating time depending on the particle/cell material. The effective gravitational force  $F_{G\sim}(\rho_P - \rho_S)R^3$  ( $\rho_P =$  density of particle/cell,  $\rho_S =$  density of solvent medium) is crucial for both particle escape from the laser beam and sedimentation back to the sample bottom. For instance, polystyrene spheres ( $\rho_P = 1.05$  g/cm<sup>3</sup>) immersed in water ( $\rho_S = 1$  g/cm<sup>3</sup>) have a low density contrast. As a consequence, the effective gravitational force is weak which hampers the ability of the particles to drop out of the laser beam. This is even exacerbated for large particles ( $R > 2$   $\mu\text{m}$ ) which are tightly trapped in the beam due to high optical gradient forces.<sup>13</sup> To circumvent this problem the laser beam is periodically switched off to aid particle escape.

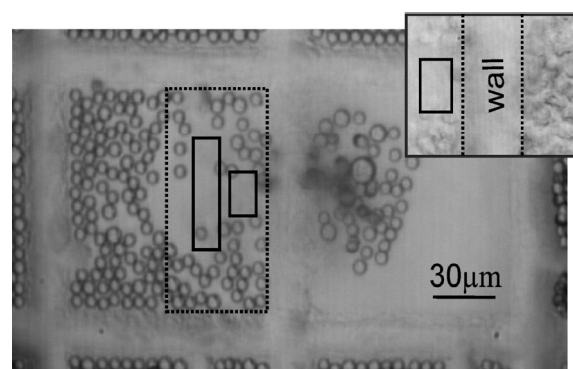


**Fig. 2** Particle and cell redistribution between microwells. Particles are guided up and over the 20  $\mu\text{m}$  PDMS wall into the neighboring microwell. A parabolic beam ( $n = 24$ ) (left solid-line rectangle) feeds the Airy beam (right solid line rectangle) with particles. Both beams are oriented rightwards. The dashed-line rectangle outlines the microwell area used for the efficiency measurements (see Fig. 3). Insert: clearing of red blood cells with an Airy beam (black rectangle) oriented to the right.

Fig. 2 shows a typical micrograph of our system at work. The Airy beam is oriented towards the right microwell, the beam size indicated by the right solid-line rectangle. The beam is operating for  $t_{\text{on},1} = 4$  s and is then switched off for  $t_{\text{off}} = 4$  s. The micrograph shows the situation  $t = 100$  s after the experiment started. The beam transported a significant fraction of particles ( $\approx 20\%$ ) over the wall and particles reappear in the right microwell. Note that the Airy beam was fed by a large parabolic beam ( $n = 24$ ), which was operating after the Airy beam for  $t_{\text{on},2} = 4$  s and the size of which is indicated by the left solid-line rectangle. Within this area the parabolic beam collects particles and conveys them towards the Airy beam which further transports them to the neighboring microwell. We have also demonstrated the transport of red blood cells as shown in the insert in Fig. 2. The region where the Airy beam operated (black frame rectangle) was cleared from cells which were transported across the wall to the right microwell (see dark shade arising from sedimenting cells). Although Fig. 2 only shows a partially cleared microwell, one only needs to sweep the entire microwell in order to fully clear it. It is also worth noting that this proof-of-concept study used a wavelength that is associated with a high absorption by cells. However, we did not observe any acute morphological changes during the course of the experiment (blebbing, granularity, *etc.*) and our approach could be easily applied to more biocompatible wavelengths ( $750$  nm  $< \lambda < 1100$  nm).

To obtain quantitative information on particle redistribution we compared the number of particles cleared by a single beam or a combination of different beams within 10 cycles of  $t_{\text{on},1} = 4$  s (first beam), then  $t_{\text{on},2} = 4$  s (second beam, feeding the first beam), and finally  $t_{\text{off}} = 4$  s. The dashed-line rectangle shown in Fig. 2 served as a reference area. The results are summarized in Fig. 3. A single Airy beam removes just less than 20% of the particles while a combination of two Airy beams transports twice this amount. The most efficient redistributing method was found to be a combination of Airy and parabolic beams. This configuration allows one to control the amount of conveyed particles between 20% and 50% for beam orders up to  $n = 18$ . Higher-order parabolic beams display a lower clearing efficiency because the distance between the two main spots becomes larger than the Airy beam size. Therefore, particles conveyed by the parabolic beam are no longer dragged by the Airy beam's side lobes.

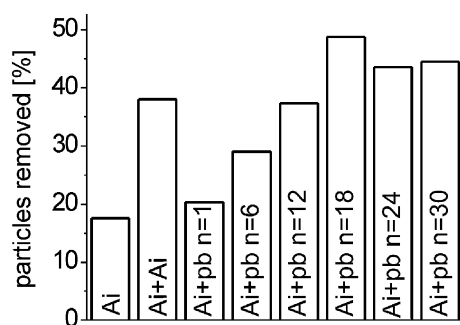


**Fig. 3** Efficiency of optically mediated particle clearing for different beams/combinations of beams (reference area indicated in Fig. 2 as dashed-line rectangle). Ai: Airy beam, pb: parabolic beam.

We also investigated how the choice of timing  $\{t_{on,1}, t_{on,2}, t_{off}\}$  affects the efficiency of particle clearing. Cycles of  $\{4\text{ s}, 4\text{ s}, 4\text{ s}\}$  turned out to be the best compromise between a short total operating time  $T$  and a large particle transport. For larger  $t_{on}$ , particles tend to jam in the beam and are levitated to larger heights; this reduces the precision of the transport direction because particles are forced out of the beam in random directions due to this jamming. For smaller  $t_{on}$ , particles are not levitated well across the wall and lots of them sediment or diffuse across the wall back into the original microwell. The same is observed for larger  $t_{off}$ . Overall, a microwell can completely be emptied in a period of  $T \approx 10\text{ min}$  through relocation of the beam(s) across the microwell.

In our studies we found that parabolic beams are less efficient than Airy beams. This can be explained as follows: As indicated by the white arrows in Fig. 1(a) (left graph) and Fig. 1(b), Airy beams and parabolic beams smear out at angles of  $135^\circ$  and  $180^\circ$  with respect to the main spot's deflection, respectively. As a consequence, optical gradient forces<sup>13</sup> become weak at these angles and particles tend to leave the main spot at these angles. In the case of the Airy beam, particles leaving the main spot are still guided towards their intended destination. In contrast, particles leaving the main spot of a parabolic beam fall in the reverse direction of their intended destination.

Another issue relates to cell transport. Although successful for red blood cells, there are general limitations for the application of this technique to other cell types. Most cell types, such as CHO cells, exhibit too little a refractive index difference with respect to the sample medium. Therefore, the light pressure forces required for cell transport are too weak.<sup>13</sup> This is exacerbated by the fact that neither an Airy nor a parabolic beam's main spot can be adjusted to  $\approx 10\ \mu\text{m}$ , the typical cell size, without considerably decreasing the curvature of the trajectory followed by the Airy beam's main spot.<sup>10</sup> A simple solution is to tag cells with dielectric spheres, which increases

the exerted light pressure forces. In phagocytotic cells such as CHO cells, tagging may be achieved simply by exposing cells to spheres.<sup>14</sup> A general solution for non-phagocytotic cell types is to antibody tag cells with microparticles.<sup>18</sup> We prepared samples containing trypsinized CHO cells which had phagocytosed polymer spheres ( $R = 1.5\ \mu\text{m}$ ) and observed successful redistribution of this cell type.

We have redistributed both microparticles and mammalian cells between PDMS microwells using curved Airy and parabolic beams. Both the size of the cleared area and the amount of the cleared particles can be controlled through the use of single or combinations of different beams. Overall our results open up an alternative route to relocate cells between different buffer media in a microfluidic chamber but notably without the presence of microfluidic flow.<sup>8</sup>

## Acknowledgements

We thank the UK EPSRC for funding and Michael Mazilu for his assistance in creating the parabolic beam phase masks. KD is a Royal Society–Wolfson Merit Award holder.

## Notes and references

- 1 K. Dholakia, P. J. Reece and M. Gu, *Chem. Soc. Rev.*, 2008, **37**, 42.
- 2 J. Durnin, J. J. Miceli and J. H. Eberly, *Phys. Rev. Lett.*, 1987, **58**, 1499.
- 3 V. Garcés-Chavez, D. McGloin, H. Melville, W. Sibbett and K. Dholakia, *Nature*, 2002, **419**, 145.
- 4 T. Cizmar, V. Garcés-Chavez, K. Dholakia and P. Zemanek, *Appl. Phys. Lett.*, 2005, **86**, 174101.
- 5 E. McLeod and C. B. Arnold, *Nature Nanotech.*, 2008, **3**, 413.
- 6 X. Tsampoula *et al.*, *Appl. Phys. Lett.*, 2007, **91**, 053902.
- 7 J. Baumgartl, M. Mazilu and K. Dholakia, *Nature Photon.*, 2008, **2**, 675.
- 8 E. Eriksson, J. Enger, B. Nordlander, N. Erjavec, K. Ramser, M. Goksör, S. Hohmann, T. Nyström and D. Hanstorp, *Lab Chip*, 2007, **7**, 71.
- 9 G. A. Siviloglou and D. N. Christodoulides, *Opt. Lett.*, 2007, **32**, 979.
- 10 G. A. Siviloglou, J. Broky, A. Dogariu and D. N. Christodoulides, *Phys. Rev. Lett.*, 2007, **99**, 213901.
- 11 M. A. Bandres, *Opt. Lett.*, 2008, **33**, 1678.
- 12 J. A. Davis, M. J. Mintry, M. A. Bandres and D. M. Cottrell, *Opt. Express*, 2008, **16**, 12866.
- 13 A. Ashkin, J. M. Dziedzic, J. E. Bjorkholm and S. Chu, *Opt. Lett.*, 1986, **11**, 288.
- 14 V. K. Kodali, W. Ross, J. P. Spatz and J. E. Curtis, *Soft Matter*, 2007, **3**, 337.
- 15 J. A. Davis, D. M. Cottrell, J. Campos, M. J. Yzuel and I. Moreno, *Appl. Opt.*, 1999, **38**, 5004.
- 16 D. Day *et al.*, *Immunol. Cell Biol.*, 2009, **87**, 154.
- 17 R. J. Clarke, K. Hognason, M. Brimacombe and E. Townes-Anderson, *Mol. Vis.*, 2008, **14**, 706.
- 18 L. Paterson, E. Papagiakoumou, G. Milne, V. Garcés-Chávez, S. A. Tatarikova, W. Sibbett, F. J. Gunn-Moore, P. E. Bryant, A. C. Riches and K. Dholakia, *Appl. Phys. Lett.*, 2005, **87**, 123901.